ORGANOMETALLICS

Article

Cite This: *Organometallics* XXXX, XXX, XXX–XXX

pubs.acs.org/Organometallics

Potent Half-Sandwich Iridium(III) and Ruthenium(II) Anticancer Complexes Containing a P^O-Chelated Ligand

Qing Du,[†] Lihua Guo,*[,†] Meng Tian,[†] Xingxing Ge,[†] Yuliang Yang,[†] Xiyan Jian,[†] Zhishan Xu,[†,‡] Zhenzhen Tian,[†] and Zhe Liu*[,†]

[†]Institute of Anticancer Agents Development and Theranostic Application, The Key Laboratory of Life-Organic Analysis and Key Laboratory of Pharmaceutical Intermediates and Analysis of Natural Medicine, Department of Chemistry and Chemical Engineering, Qufu Normal University, Qufu 273165, People's Republic of China

[‡]Department of Chemistry and Chemical Engineering, Shandong Normal University, Jinan 250014, People's Republic of China

Supporting Information

ABSTRACT: We herein report the synthesis, characterization, and anticancer activity of a series of iridium(III) and ruthenium(II) half-sandwich complexes of the type $[(Cp^x/arene)M(P\text{^}O)Cl]PF_6$ (M = Ir, Cp^x = pentamethylcyclopentadienyl (Cp*) or its phenyl (Cp^{xph} = $C_5Me_4C_6H_5$) or biphenyl (Cp^{xbiph} = $C_5Me_4C_6H_4C_6H_5$) derivatives; M = Ru, arene = *p*-cymene (*p*-cym); P^O = phosphine phosphonic amide ligand (PPOA)). The X-ray crystal structures of all complexes, in which the ligand can form six-membered rings with the metal center, have been determined. All of the complexes show remarkable anticancer activities toward HeLa and A549 cancer cells, activities which are higher than that of the clinical anticancer drug cisplatin. The incorporation of phenyl substituents on the Cp* ring for iridium(III) complexes results in little variation in their anticancer activities. These results can be attributed to the combinatorial action of the metal and PPOA ligand. Hydrolysis and DNA cleavage are not the major mechanisms of action. These complexes show potent catalytic activity in the transfer hydrogenation of NADH to NAD^+. Additionally, complexes $[(\eta^5\text{-}C_5Me_5)Ir(P\text{^}O)Cl]PF_6$ (**1**) and $[(\eta^6\text{-}p\text{-cym})Ru(P\text{^}O)Cl]PF_6$ (**4**) arrest cell cycles at S and G_2/M phase and S phase, respectively. Complexes **1** and **4** both can induce apoptosis of HeLa cancer cells. Reactive oxygen species (ROS) and mitochondrial membrane potential tests were also performed to explore the mechanism of action. When the concentration of the complexes is increased, the amount of reactive oxygen species (ROS) increases dramatically and the mitochondrial membrane potential decreases significantly in HeLa cancer cells. Overall, cell stress including cell cycle perturbation, apoptosis induction, increase in ROS level, and loss of mitochondrial membrane potential contributes to the anticancer potency of these complexes. Interestingly, the use of confocal microscopy provides insights into the microscopic mechanism in which the typical and most active complex **1** can damage lysosomes. This type of complex represents a potent platform for development of metal anticancer drugs.

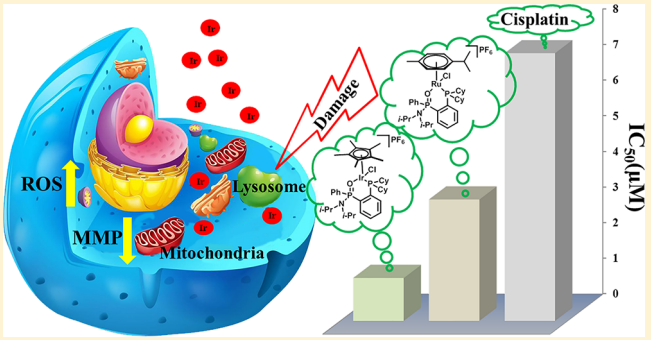

INTRODUCTION

The clinical success of platinum-based anticancer agents has stimulated the exploration for other metal-based diagnostic and chemotherapeutic drugs, which may be able to reduce side effects, widen the spectrum of sensitive tumors, and overcome platinum resistance.[1] Among these metallodrugs, organometallic iridium(III) and ruthenium(II) complexes offer rich versatility for the rational design of anticancer agents.[2] In a search for these complexes as potent chemotherapeutic compounds, many different fixed ligands such as η^5-C_5Me_5 and η^6-arene have been used in combination with monodentate ligands[3] and bidentate cationic or neutral C,N-,[4] N,N-,[5] N,O-,[5a,6] P,P-,[3c,7] and P,S-ligands.[8] In particular, iridium(III) and ruthenium(II) complexes containing phosphorus ligands have emerged as promising anticancer agents and even are advancing to clinical trials. For example, complex **I** (Scheme 1) containing a monodentate amphiphilic phosphorus ligand shows excellent antimetastatic and antiangiogenic behavior in vivo and is able to reduce the growth of certain primary tumors.[3a] Our group has reported types of half-sandwich iridium(III) and ruthenium(II) complexes with 2,20-bis(diphenylphosphino)-1,10-binaphthyl (BINAP) as a P,P-chelating ligand and showed that the cytotoxicity of the complexes may be associated with the redox mechanism of action (**II**, Scheme 1).[7] Broomfield et al. also have highlighted the potential utility of the bis-phospinoamine scaffold as an easily tunable auxiliary ligand core in a logical design of anticancer agents (**III**, Scheme 1).[3c] In addition, Ludwig et al. have developed a series of half-sandwich ruthenium(II)

Received: June 11, 2018

DOI: 10.1021/acs.organomet.8b00402
Organometallics XXXX, XXX, XXX–XXX

Scheme 1. Reported Half-Sandwich Iridium(III) and Ruthenium(II) Anticancer Complexes I–IV Containing Phosphorus Ligands and Our Current Work

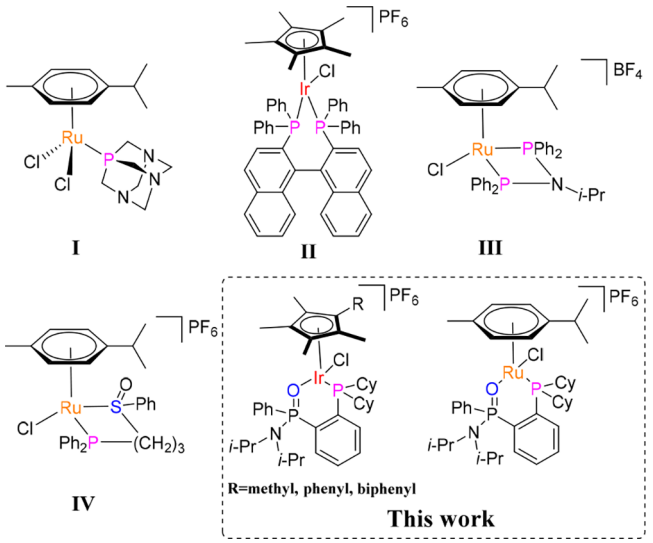

complexes containing P,S-ligands (**IV**, Scheme 1). These complexes displayed high biological potential even against cisplatin-resistant tumor cell lines.[8b] On the other hand, P,O-chelating ligands are currently receiving much attention for their versatile structures and wide applications in the field of coordination chemistry and catalysis.[9] The most distinguishing feature of this class of electronically nonsymmetric neutral ligand is the combination of a very strongly σ donating phosphine moiety and a very weakly σ donating oxygen moiety. These studies encouraged us to prepare a series of half-sandwich iridium(III) and ruthenium(II) complexes bearing phosphine phosphonic amide ligands and explore their anticancer activity and reactivity toward biomolecules.

For this work, the phosphine phosphonic amide ligand was chosen to prepare new iridium(III) and ruthenium(II) half-sandwich complexes. These complexes have been systematically investigated for their chemical and biological reactivity and cancer cell toxicity against HeLa and A549 cancer cells. Flow cytometry experiments, including cell cycle, apoptosis induction, ROS level, and mitochondrial membrane potential, were carried out to explore the mechanism of action. In particular, confocal microscopy was employed to investigate the lysosome damage.

RESULTS AND DISCUSSION

Synthesis and Characterization of Complexes 1–4. The phosphine phosphonic amide ligand was previously synthesized and used as a supporting ligand for palladium-catalyzed organic Suzuki–Miyaura cross-coupling reactions[10] and ethylene polymerization.[9] However, the iridium(III) and ruthenium(II) complexes based on this ligand have never been prepared or studied in bioinorganic chemistry. $[(\eta^5\text{-}C_5Me_5)IrCl_2]_2$ (dimer 1), $[(\eta^5\text{-}C_5Me_4C_6H_5)IrCl_2]_2$ (dimer 2), $[(\eta^5\text{-}C_5Me4C_6H_4C_6H_5)IrCl_2]_2$ (dimer 3), $[(\eta^6\text{-}p\text{-cym})RuCl_2]_2$ (dmer 4), and phosphine phosphonic amide (PPOA) ligand were synthesized according to previously reported procedures.[9b,10,11] The reactions between the ligand PPOA and the corresponding dimers were carried out in CH_3OH at ambient temperature and led to complexes **1–4** in 51–75% yields (Scheme 2). These newly synthesized compounds were all isolated as PF_6^- salts and characterized by ^1H NMR, ^{13}C NMR, mass spectroscopy, and elemental analysis.

X-ray Crystal Structures. Crystals of complexes **1–4** suitable for X-ray diffraction were obtained from a slow diffusion of diethyl ether into dichloromethane solutions of the complexes at room temperature (Figure 1). X-ray crystallographic data are given in Table S1 (see the Supporting Information), and selected bond lengths and angles are summarized in Table S2 (see the Supporting Information). As expected, these complexes adopt a pseudo-octahedral "piano-stool" geometry with Cp^x or *p*-cym acting as theseat and the bidentate phosphine phosphonic amide ligand and a monodentate chloride acting as the legs. In all cases, the metal center is part of a six-membered (PO)Ir or (PO)Ru chelate ring system. Generally, the Ir–P and Ru–P bond distances (2.325–2.367 Å) are slightly longer than the Ir–O and Ru–O bond distances (2.097–2.157 Å). The Ir–Cl bond distances are 2.3925(12), 2.3913(16), and 2.394(2) Å for **1–3**, respectively, and the Ru–Cl bond distance is 2.3878(11) Å for **4**. No intermolecular π–π stacking in the unit cell is observed in these crystal structures.

In Vitro Cytotoxicity. The cytotoxicities of complexes **1–4** toward HeLa human cervical cancer cells were investigated by an MTT assay. The IC_{50} values (concentration at which 50% of the cell growth is inhibited) after 24 h of exposure to the compounds are shown in Table 1 and Figure 2. Interestingly, these new complexes are highly potent toward the human HeLa cervical cancer cell line and the lung cancer A549 cell line with IC_{50} values of 1.2–3.8 and 4.4–7.5 μM, respectively. The IC_{50} values of these complexes are much lower than the values obtained with cisplatin against HeLa cells (1.2–3.8 μM vs 7.5 μM) and A549 cells (4.4–7.5 μM vs 21.3 μM).

Scheme 2. Synthesis of Complexes 1–4

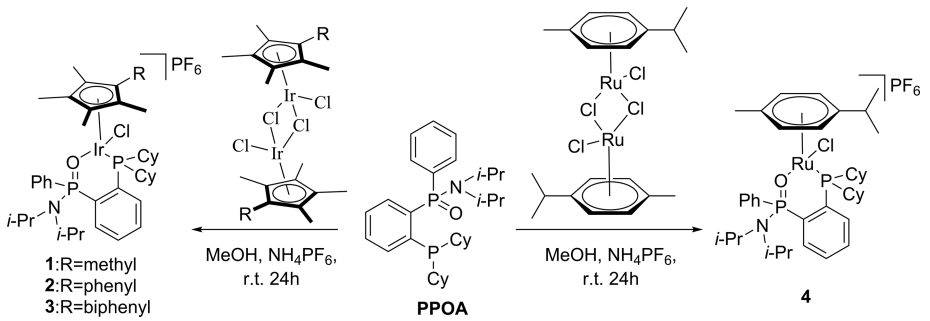

DOI: 10.1021/acs.organomet.8b00402
Organometallics XXXX, XXX, XXX–XXX

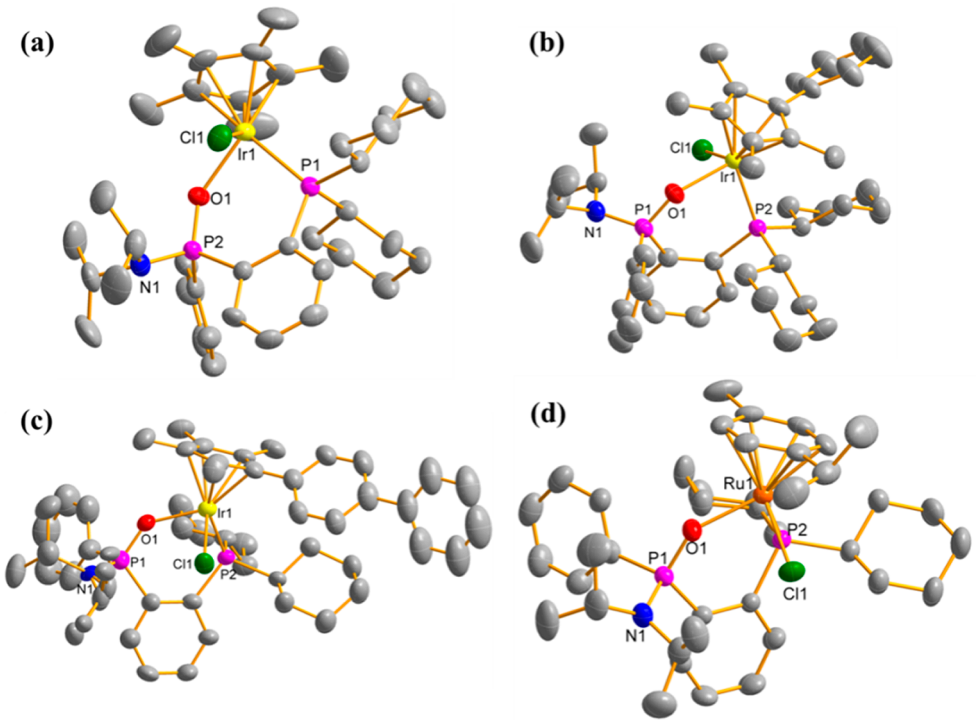

Figure 1. X-ray crystal structures with atom numbering schemes for (a) complex **1**, (b) complex **2**, (c) complex **3**, and (d) complex **4** with the thermal ellipsoids drawn at the 50% probability level. The hydrogen atoms and PF_6^- anion have been omitted for clarity. Selected bond lengths (Å): complex **1**, Ir−C(centroid) = 1.814, Ir−O = 2.137(3), Ir−P = 2.3315(12), Ir−Cl = 2.3925(12); complex **2**, Ir−C(centroid) = 1.817, Ir−O = 2.157(4), Ir−P = 2.3265(14), Ir−Cl = 2.3913(16); complex **3**, Ir−C(centroid) = 1.828, Ir−O = 2.147(5), Ir−P = 2.325(2), Ir−Cl = 2.394(2); complex **4**, Ru−C(centroid) = 1.7018, Ru−O = 2.097(3), Ru−P = 2.3672(12), Ru−Cl = 2.3878(11).

Table 1. IC_{50} Values of Complexes 1−4 Tested toward Cancer and Normal Cell Lines and Comparison with Cisplatin[a]

	IC_{50} (μM)			
complex	HeLa	A549	BEAS-2B	16HBE
$[(\eta^5\text{-}C_5Me_5)Ir(P\text{^}O)Cl]PF_6$ (**1**)	1.2 ± 0.1	4.9 ± 1.2	1.3 ± 0.2	1.9 ± 0.2
$[(\eta^5\text{-}C_5Me_4C_6H_5)Ir(P\text{^}O)Cl]PF_6$ (**2**)	3.8 ± 0.2	4.4 ± 0.4	3.5 ± 0.1	4.5 ± 0.2
$[(\eta^5\text{-}C_5Me_3C_6H_4C_6H_5)Ir(P\text{^}O)Cl]PF_6$ (**3**)	1.6 ± 0.3	7.5 ± 1.1	2.8 ± 0.4	3.0 ± 0.1
$[(\eta^6\text{-}p\text{-cym})Ru(P\text{^}O)Cl]PF_6$ (**4**)	3.4 ± 0.4	5.0 ± 0.1	4.9 ± 1.2	5.3 ± 0.9
PPOA	>50	>50	*b*	
dimer 1	>50	>50		
dimer 2	>50	>50		
dimer 3	>50	>50		
dimer 4	>50	>50		
cisplatin	7.5 ± 0.2	21.3 ± 1.7		

[a]Data are presented as means ± standard deviations. [b]Not determined.

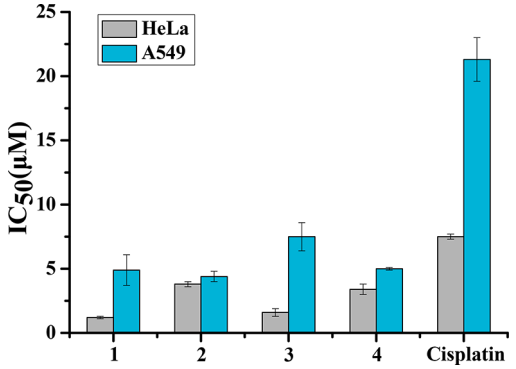

Figure 2. Inhibition of the growth of HeLa and A549 cells by complexes **1**-**4** and cisplatin.

Otherwise, the PPOA ligand and four precursor dimers show very low cytotoxicity against HeLa cells and A549 cells (>50 μM). In particular, as far as we know, most of the cytotoxic organometallic ruthenium(II) compounds generally tend to be less potent than cisplatin.[3b,12] However, the ruthenium(II) complex **4** in this system displays a potency higher than that of cisplatin, which can be attributed to the combinatorial action of the metal and PPOA ligand. Further, in contrast to the reported half-sandwich C,N and N,N-chelating iridium(III) complexes,[5b,13] the presence of the extended phenyl rings in this system only slightly changes the anticancer activity of the complexes. Generally, the hydrophobicity and intercalative ability of extended cyclopentadienyl systems make the major contribution to the anticancer activity of half-sandwich C,N and N,N-chelating iridium(III) complexes.[4d] In this system, the major role of the chelating ligand PPOA may have offset

DOI: 10.1021/acs.organomet.8b00402
Organometallics XXXX, XXX, XXX−XXX

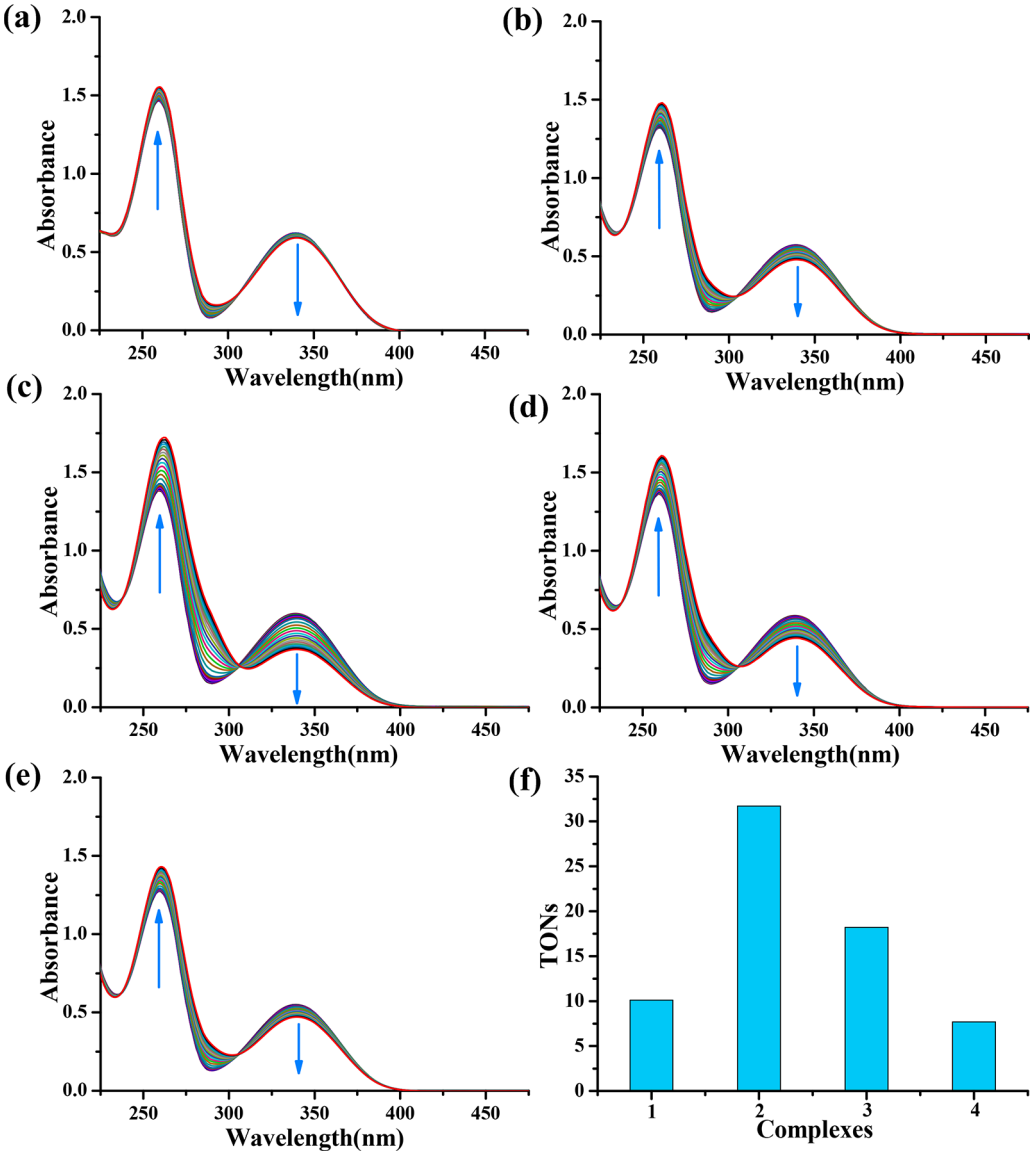

Figure 3. UV−vis spectra of the reaction of NADH (87 μM) with complexes **1**−**4** (0.8 μM) in 5% MeOH/95% H_2O (v/v) at 298 K for 8 h: (a) control: only NADH; (b) complex **1** + NADH; (c) complex **2** + NADH; (d) complex **3** + NADH; (e) complex **4** + NADH. (f) Turnover numbers (TONs) of complexes **1**−**4**.

the advantages of having the extended arenes on the Cp*. Considering the aforementioned high anticancer activity of ruthenium(II) complex **4**, this is highly speculative at this point. Furthermore, the investigated iridium(III) and ruthenium(II) complexes have been shown to interfere with mitochondrial activity (see below, in Effect on Mitochondrial Membrane Potential (MMP)) so that the metabolization of MTT can reflect an effect of metal complexes on the mitochondrial metabolism rather than the viability of the cell. Thus, a cell viability assay was also determined by colorimetric assays based on neutral red (Table S3 in the Supporting Information). There is no significant difference from the results of the MTT assay, indicating that the MTT test is only slightly affected by changes in the mitochondrial metabolism.

The cytotoxicities of complexes **1**−**4** were further evaluated against the two human bronchial epithelial normal cells BEAS-2B and 16HBE (Table 1). Unfortunately, no selectivity was observed for cancer cells versus normal cells with these complexes. Hence, more structural modification is necessary in future work to decrease the cytotoxic action toward normal cells without loss of the selectivity between cancer and normal cells.

Hydrolysis Studies. Hydrolysis of M−Cl bonds is considered to be an activation step for half-sandwich transition-metal analogues.[5a,14] M−OH_2 aqua complexes are often more reactive than the corresponding chloride complexes.[5a] For the investigation of aqueous stability, studies were conducted by ^{1}H NMR spectroscopy for complexes **1** and **4**, which were dissolved in 85% MeOD-d_4/15% D_2O (v/v) or in 70% DMSO-d_6/30% D_2O (v/v). The presence of methanol or DMSO ensured the solubility of the complexes. The ^{1}H NMR spectra of **1** and **4** showed no obvious change over 24 h (Figures S13−S16 in the Supporting Information). It is possible that the aqua complex was obtained before the ^{1}H NMR spectra were acquired. Therefore, NaCl (32 mol equiv) was then added to the solutions to further confirm the hydrolysis of these complexes. There was also no change in the

DOI: 10.1021/acs.organomet.8b00402
Organometallics XXXX, XXX, XXX−XXX

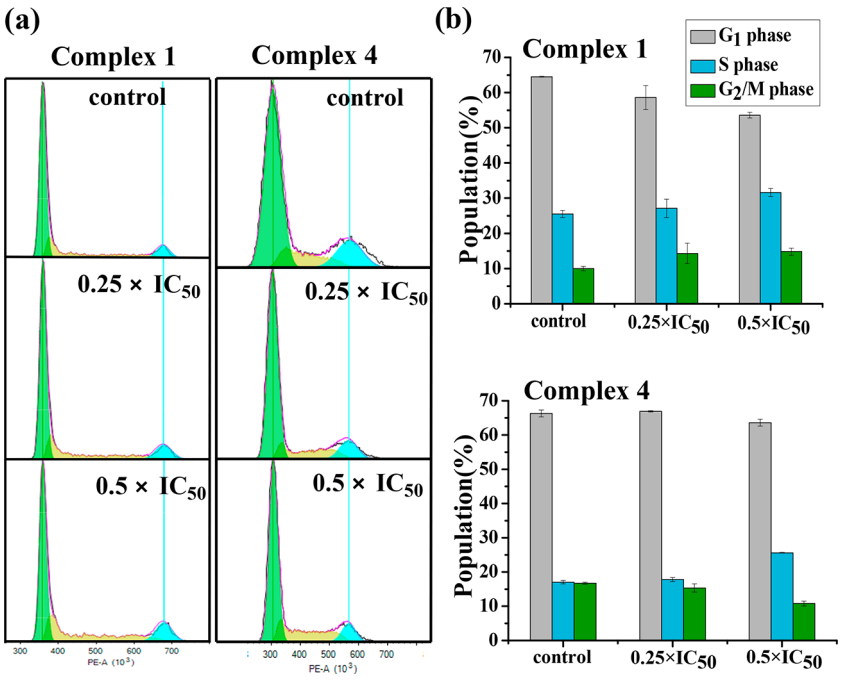

Figure 4. Cell cycle analysis of HeLa cancer cells after 24 h of exposure to complexes **1** and **4** at 310 K. The concentrations used were 0.25 and 0.5 equipotent concentrations of IC_{50}. Cell staining for flow cytometry was carried out using PI/RNase. (a) FL2 histogram for the negative control (untreated cells) and complexes **1** and **4** with 0.25 and 0.5 equipotent concentrations of IC_{50}. (b) Cell populations in each cell cycle phase for control and complexes **1** and **4**. Data are quoted as mean ± SD of three replicates.

^{1}H NMR spectra. These results suggest that the complexes remained stable under these conditions.

It should be noted that some previously reported half-sandwich metal complexes may undergo Cl^-/H_2O exchange more easily in dilute solutions with a higher relative content of water, as is the case of cell culture.[3b,15] As a result, the hydrolysis behaviors of complexes **1** and **4** in 35% MeOH/65% H_2O (v/v) and complexes **2** and **3** in 10% MeOH/90% H_2O (v/v) were also monitored by UV−vis at 298 K. No absorbance changes were observed in UV−vis spectra (Figure S17 in the Supporting Information). Meanwhile, the hydrolysis behaviors of complexes **1** and **4** in 30% DMSO/70% H_2O (v/v) or 30% DMSO/70% PBS (v/v) were also monitored by UV−vis at 298 K. No absorbance changes were observed in UV−vis spectra (Figures S18 and S19 in the Supporting Information), which indicated that the hydrolysis also did not occur when a high content of water was employed. As a result, the stability studies suggest that the compounds have sufficient stability for the preparation of samples for biological assays.

Interaction with Nucleobases. DNA often represents a primary target site for many transition-metal anticancer complexes.[16] Thus, the binding of 9-methyladenine (9-MeA) and 9-ethylguanine (9-EtG) to complexes **1** and **4** was studied. The addition of 1 mol equiv of 9-MeA or 9-EtG to an equilibrium solution of **1** and **4** (0.5 mM) in 85% MeOD-d_4/15% D_2O (v/v) at 310 K resulted in no additional ^{1}H NMR peaks over a period of 24 h (Figures S20−S23 in the Supporting Information), suggesting that no reaction with 9-EtG and 9-EtA occurred in this system. In addition, the formation of nucleobase adducts by these iridium(III) and ruthenium(II) complexes was not detected by mass spectrometry. These results indicate that DNA may not be the main target for these iridium(III) and ruthenium(II) P^O anticancer complexes.

Plasmid DNA Cleavage. In order to assess the DNA cleavage ability of these complexes, plasmid pBR322 DNA (10 μM) was incubated with complexes **1** and **4** (0−100 μM) for 24 h and was monitored using agarose gel electrophoresis in a buffer (40 mM Tris-HCl/1 mM EDTA, pH 8.3). However, no DNA cleavage was observed for these complexes even at a concentration of 100 μM (Figure S24 in the Supporting Information). These results further confirm that DNA is not a pharmacological target for these complexes.

Reaction with NADH. Coenzymes nicotinamide adenine dinucleotide NADH and NAD^+ play a crucial role in numerous biocatalyzed processes. Previously, the Sadler group reported that NADH can donate a hydride to aqua iridium cyclopentadienyl complexes and produce ROS in the form of H_2O_2, thus providing a pathway to an oxidant mechanism of action.[17] As a result, the catalytic transfer hydrogenation behavior of complexes **1**−**4** with coenzyme NADH was also investigated. To evaluate the real catalytic activity, we incubated 87 μM NADH in a solution of 5% MeOH/95% H_2O (v/v) as a control. The reaction of complexes **1**−**4** (ca. 0.8 μM) with NADH (87 μM) in 5% MeOH/95% H_2O (v/v) was monitored by UV−vis at 298 K after various time intervals. It is simple to measure the conversion of NADH to NAD^+ by measuring the amount of UV absorption at 339 nm, as NADH has an absorption at 339 nm while NAD^+ does not.[17] The turnover numbers (TONs) of complexes calculated by the amount of UV absorption at 339 nm (Figure 3) revealed the following trends in catalytic activity: **1** (10.1), **2** (31.7), **3** (18.2), and **4** (7.7), **2** > **3** > **1** > **4**. Despite no clear trend being observed, it is apparent that the presence of a ruthenium metal center seems to reduce the catalytic activity. As these complexes can convert NADH to NAD^+, the catalytic performance may provide a potential pathway to induce ROS and enhance the killing of cancer cells by an oxidant mechanism of action.[17c]

DOI: 10.1021/acs.organomet.8b00402
Organometallics XXXX, XXX, XXX−XXX

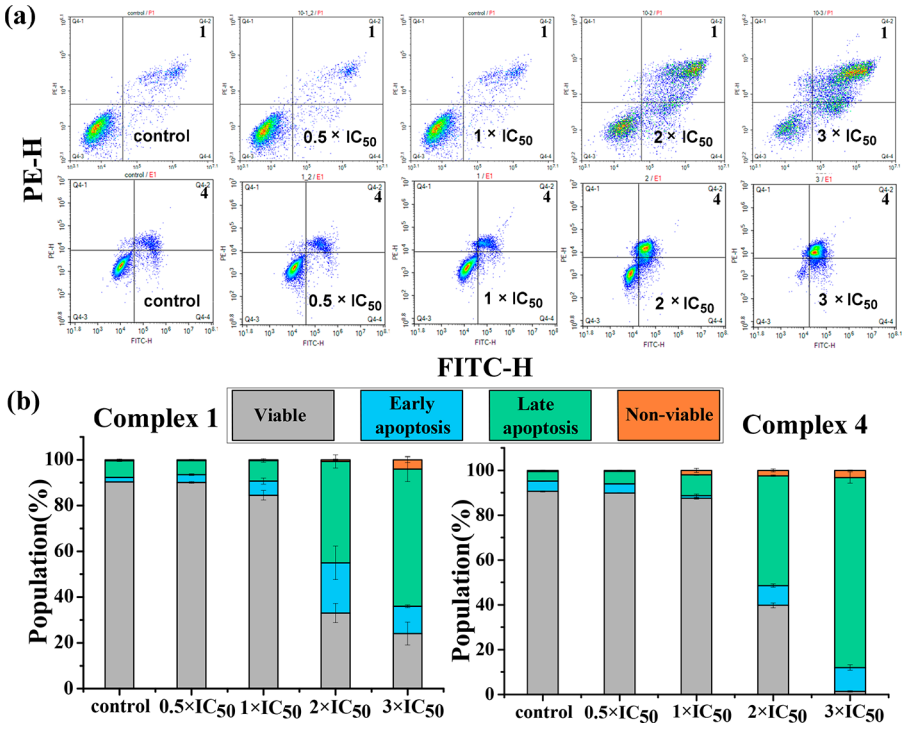

Figure 5. Apoptosis analysis of HeLa cells after 24 h of exposure to complexes **1** and **4** at 310 K determined by flow cytometry using annexin V-FITC vs PI staining. (a) HeLa cells left untreated (control) or treated with different concentrations of complexes **1** and **4** for 24 h. (b) Histogram showing populations for HeLa cells in four stages treated by complexes **1** and **4**. Data are quoted as mean ± SD of three replicates.

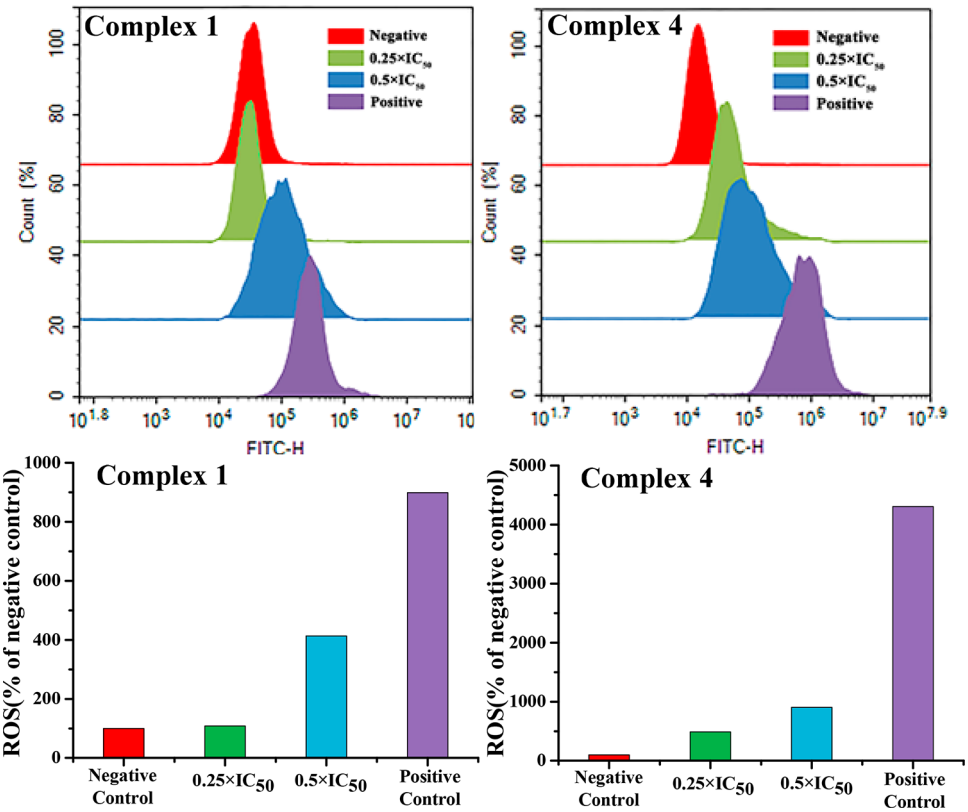

Figure 6. Analysis of ROS level by flow cytometry after HeLa cells were treated with complexes **1** and **4** at 0.25 and 0.5 equipotent concentrations of IC_{50} for 24 h and stained with H_2DCFDA. Data are quoted as mean ± SD of three replicates.

Cellular-Metal Accumulation. As iridium and ruthenium are exogenous elements, the cellular uptake levels of Ir(III) and Ru(II) can be quantitatively determined by inductively coupled plasma mass spectrometry (ICP-MS). HeLa cells were incubated with 5 μM complexes **1**−**4** for 6 h. The intracellular metal content induced by incubation of these

DOI: 10.1021/acs.organomet.8b00402
Organometallics XXXX, XXX, XXX−XXX

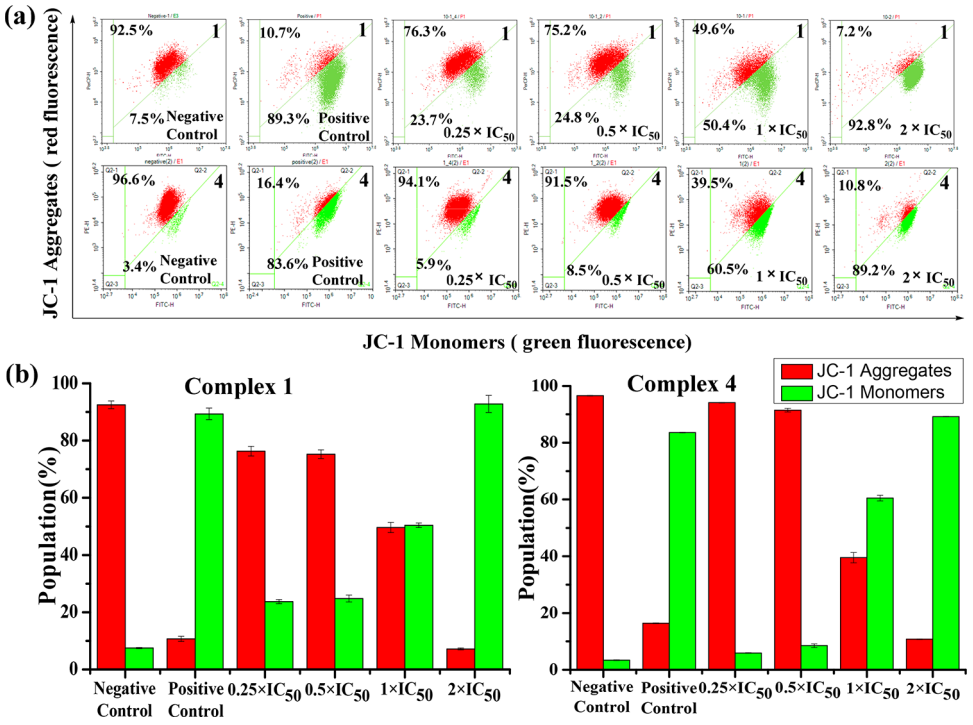

Figure 7. Changes in mitochondrial membrane potential of HeLa cancer cells induced by complexes **1** and **4**. (a) Flow cytometry histograms of the changes induced by the complexes **1** and **4** at concentrations of 0.25 × IC_{50}, 0.5 × IC_{50}, 1 × IC_{50}, and 2 × IC_{50}. (b) Populations of cells that exhibit a reduction in the mitochondrial membrane potential. Data are quoted as mean ± SD of three replicates.

complexes is in the range of 78−90 ppb per 1 × 10^5 cells (Figure S25 in the Supporting Information). In comparison to complex **1**, complex **3** showed a higher level of intracellular iridium content (90 ppb per 1 × 10^5 cells vs 78 ppb per 1 × 10^5 cells). This result is most likely due to the extended phenyl rings in complex **3**, which increase its lipophilicity and thus enhance the cell membrane penetration. However, the differences in the levels of cellular-metal accumulation are small. This can be also attributed to the major role of the PPOA ligand in this system.

Cell Cycle Arrest. Cell cycle arrest analysis for complexes **1** and **4** toward HeLa cells was also performed by flow cytometry to confirm whether the induced cell growth inhibition was the result of cell cycle arrest. The treatment of HeLa cells with complex **1** at 0.5 × IC_{50} concentration led to mainly S and G_2/M phase arrest, where the percentages of cells increased from 25.5% and 10.0% to 31.6% and 14.8%, respectively, in comparison to untreated cells. On the other hand, complex **4** blocked the cell cycle at S phase, where the percentages of cells showed an increase from 17.0% to 25.6% under the same test conditions (Figure 4 and Tables S4 and S5 in the Supporting Information). These results suggested that the anticancer mechanism of **1** and **4** on HeLa cells is dominantly S and G_2/M phase arrest in a concentration-dependent manner.

Apoptosis Assay. Apoptosis is a programmed cell death process, and it has been reported to inhibit cell growth by activating apoptosis for a large number of transition-metal-based anticancer drugs.[18] Complexes **1** and **4** were selected for further biological investigation on their mechanism of action. In order to investigate whether the reduction in cell viability observed in the MTT assay is based on apoptosis, HeLa cells were treated with complexes **1** and **4** at 0.5, 1, 2, and 3 equipotent concentrations of IC_{50} for 24 h and then stained with annexin V/propidium iodide and analyzed by flow cytometry. This allowed determination of cell populations as viable (unstained, only self-fluorescence), early apoptosis (stained by annexin V only, green fluorescence), late apoptosis (stained by annexin V and PI, green and red fluorescence), and nonviable (stained by PI only, red fluorescence). As shown in Figure 5 and Tables S6 and S7 (see the Supporting Information), when HeLa cells were incubated with complexes **1** and **4** at 3 × IC_{50} concentration, totals of 71.9% and 95.4% (early apoptotic + late apoptotic) of the cells were undergoing apoptosis, respectively. Notably, the most apoptotic cells were in late apoptosis stage. In addition, because active caspase 3 is a common effector in several apoptotic pathways, it is a good marker to detect apoptotic cells by flow cytometry.[19] At a time of 24 h after the treatment of complex **4**, 11.3% of active caspase 3-positive cells was detected, which was significantly higher than the percentage (1.2%) in untreated HeLa cells (Figure S26 in the Supporting Information). This result further confirmed that these complexes can induce cell death mainly through the apoptotic pathway.

ROS Determination. Reactive oxygen species (ROS) play important roles in regulating cell proliferation, death, and signaling, even in the mechanism of action of anticancer agents.[13] The levels of reactive oxygen species in HeLa cancer cells induced by complexes **1** and **4** were determined by flow cytometry analysis (Figure 6). When HeLa cancer cells were exposed to complexes **1** and **4** for 24 h, increased and concentration-dependent ROS total levels (combined levels of H_2O_2, peroxy, hydroxyl radicals, peroxynitrite, and NO) in the cells were observed. It should be noted that similar half-sandwich C,N-chelating iridium anticancer complexes generating the ROS H_2O_2 by catalytic hydride transfer from the coenzyme NADH to oxygen has been reported previously.[17c] In addition, as mentioned above, the conversion of NADH to NAD^+ by these complexes was also observed in this system. As

DOI: 10.1021/acs.organomet.8b00402
Organometallics XXXX, XXX, XXX−XXX

a result, H_2O_2 production was further determined. We observed an increase in the H_2O_2 levels in cells treated with complex **1** or complex **4** in comparison to untreated cells (Figure S27 in the Supporting Information). Moreover, in this system, the main type of ROS was H_2O_2, which accounted for ca. 60% of the total ROS levels. The increased ROS level for these complexes played an important role in their anticancer activity and thus was also deemed as the mechanism of action in this system.

Effect on Mitochondrial Membrane Potential (MMP). The mitochondrion is the bioenergetic center of the cell, and more importantly, it is also an essential component of the intrinsic apoptotic signaling pathway. Once the membrane integrity of mitochondria is destroyed, the pro-death factors are released from mitochondria and initiate the death signaling cascade. In addition, mitochondrial dysfunction can induce cell death. Mitochondrial dysfunction can be assessed by measuring changes in mitochondrial membrane potential ($\Delta\Psi_m$).[20] Analysis of the $\Delta\Psi_m$ values in HeLa cancer cells after exposure to complexes **1** and **4** (at concentrations of 0.25, 0.5, 1, and 2 × IC_{50}) was carried out by observing the fluorescence of JC-1 (an ideal fluorescent probe widely used to detect mitochondrial membrane potential) using flow cytometry (Figure 7). When the concentration of complexes **1** and **4** was increased, the mitochondrial membrane potential decreased significantly in HeLa cancer cells. For example, when the concentration of the complex **1** was increased from 0.25 × IC_{50} to 2 × IC_{50}, the percentage of cells with mitochondrial membrane depolarization increased from 23.7% to 92.8% (Tables S8 and S9 in the Supporting Information). The ζ potentials of complex **1** (8.9 ± 0.6) and complex **4** (6.3 ± 0.5) were positively charged, which could contribute to binding of negatively charged mitochondria after entering the cytosol (Figure S28 in the Supporting Information). As a result, these complexes can induce cancer cell death through the dysfunction of the mitochondrial membrane potential.

Lysosomal Damage. Acridine orange (AO) is an effective probe used to measure the functional state of the acidic organelles, due to its characteristic of emitting red fluorescence at high concentrations in lysosomes and green fluorescence at low concentrations in the cytosol and the nucleus.[21] Therefore, the lysosomal integrity of HeLa cells was observed by AO staining. As shown in Figure 8, HeLa cells treated with acridine orange (AO) alone displayed distinct red fluorescence in lysosomes. However, the red fluorescence of AO significantly decreased with an increase in drug concentration, suggesting that lysosomal integrity was damaged under the treatment of complex **1**. It seems reasonable that, in accordance with the behavior of some previously reported potent anticancer agents,[22] the introduction of nitrogen-containing groups (−N(*i*-Pr)$_2$) to these complexes may increase the total basicity of the molecule and further result in the accumulation and damage in acidic lysosomes. Therefore, we conclude that complex **1** can induce apoptosis through lysosomal damage.

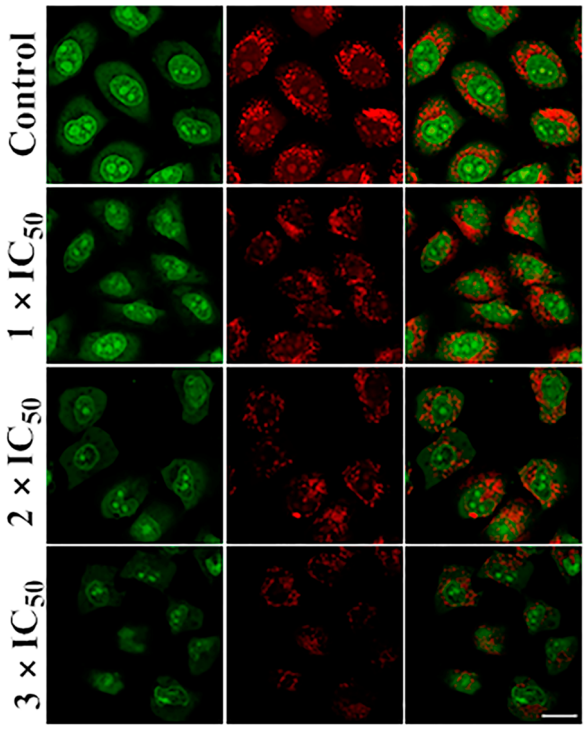

Figure 8. Observation of lysosomal disruption in HeLa cells loaded with complex **1** for 12 h at 37 °C and then stained with acridine orange (AO) (5 μM) at 37 °C for 15 min. Emission was collected at 510 ± 20 nm (green) and 625 ± 20 nm (red) upon excitation at 488 nm. Scale bar: 20 μm. The HeLa cells were treated with acridine orange (AO), acridine orange (AO) and complex **1** (1× IC_{50}), acridine orange (AO) and complex **1** (2 × IC_{50}), and acridine orange (AO) and complex **1** (3 × IC_{50}), respectively.

CONCLUSIONS

A series of PPOA-based half-sandwich iridium(III) and ruthenium(II) anticancer complexes have been prepared and fully characterized. The X-ray crystal structures of all complexes, in which the ligand can form six-membered rings with the metal center, have been determined. All the complexes display higher potency toward HeLa and A549 human cancer cells in comparison to the clinical anticancer drug cisplatin. The presence of the extended phenyl rings in this system only slightly changed the anticancer activity of the complexes. These results can be attributed to the combinatorial action of metal and PPOA ligand. These types of iridium(III) and ruthenium(II) complexes could be promising candidates to build potential anticancer agents for future cancer therapy. Several conclusions can be drawn from chemical reactivity and biological activity studies for these complexes.

(1) Hydrolysis and DNA cleavage were not the major mechanisms of action. The ^{1}H NMR spectra and UV−vis spectra of these complexes showed that no hydrolysis occurs and that the complexes remain stable under these conditions. No nucleobase binding or DNA cleavage was observed for these types of complexes under the conditions mentioned in the experiment, suggesting that DNA is not a possible target.

(2) The mechanism of action (MoA) of these complexes is attributed to cell stress including cell cycle perturbation, apoptosis induction, increase of ROS level, and loss of mitochondrial membrane potential. For example, complexes **1** and **4** arrested the cell cycle at S and G_2/M phase, induced obvious cell apoptosis and high increase in the level of ROS in HeLa cancer cells, and aroused a decrease in mitochondrial membrane potential.

(3) The generation of the ROS H_2O_2 in this system arises from catalytic hydride transfer from the coenzyme NADH to oxygen. In addition, these complexes may induce apoptosis through lysosomal damage.

DOI: 10.1021/acs.organomet.8b00402
Organometallics XXXX, XXX, XXX−XXX

■ ASSOCIATED CONTENT

Supporting Information

TThe Supporting Information is available free of charge on the ACS Publications website at DOI: 10.1021/acs.organomet.8b00402.

Experimental section and Figures S1−S28 and Tables S1−S9 as described in the text (PDF)

Accession Codes

CCDC 1565352, 1565354−1565355, and 1815607 contain the supplementary crystallographic data for this paper. These data can be obtained free of charge via www.ccdc.cam.ac.uk/data_request/cif, or by emailing data_request@ccdc.cam.ac.uk, or by contacting The Cambridge Crystallographic Data Centre, 12 Union Road, Cambridge CB2 1EZ, UK; fax: +44 1223 336033.

■ AUTHOR INFORMATION

Corresponding Authors

*E-mail for L.G.: guolihua@qfnu.edu.cn.

*E-mail for Z.L.: liuzheqd@163.com.

ORCID

Lihua Guo: 0000-0002-0842-9958

Zhe Liu: 0000-0001-5796-4335

Notes

The authors declare no competing financial interest.

■ ACKNOWLEDGMENTS

We thank the Shandong Provincial Natural Science Foundation (ZR2018MB023), the National Natural Science Foundation of China (Grant Nos. 21671118 and 21706147), the Taishan Scholars Program, the Key Laboratory of Polymeric Composite & Functional Materials of the Ministry of Education (PCFM-2017-01), and the excellent experiment project of Qufu Normal University (jp201705) for support. We thank Juanjuan Li for stimulating discussions.

■ REFERENCES

(1) (a) Hartinger, C. G.; Dyson, P. J. Bioorganometallic chemistry−from teaching paradigms to medicinal applications. *Chem. Soc. Rev.* **2009**, *38*, 391−401. (b) Gasser, G.; Ott, I.; Metzler-Nolte, N. Organometallic anticancer compounds. *J. Med. Chem.* **2011**, *54*, 3−25. (c) Che, C. M.; Siu, F. M. Metal complexes in medicine with a focus on enzyme inhibition. *Curr. Opin. Chem. Biol.* **2010**, *14*, 255−261. (d) Ronconi, L.; Sadler, P. J. Using coordination chemistry to design new medicines. *Coord. Chem. Rev.* **2007**, *251*, 1633−1648. (e) Allardyce, C. S.; Dyson, P. J. Metal-based drugs that break the rules. *Dalton Trans* **2016**, *45*, 3201−3209. (f) He, X. D.; Tian, M.; Liu, X. C.; Tang, Y. H.; Shao, C. F.; Gong, P. W.; Liu, J. F.; Zhang, S. M.; Guo, L. H.; Liu, Z. Triphenylamine-appended half-sandwich iridium(III) complexes and their biological applications. *Chem. - Asian J.* **2018**, *13*, 1500−1509.

(2) (a) Liu, Z.; Sadler, P. J. Organoiridium complexes: anticancer agents and catalysts. *Acc. Chem. Res.* **2014**, *47*, 1174−1185. (b) Liu, H. K.; Sadler, P. J. Metal complexes as DNA intercalators. *Acc. Chem. Res.* **2011**, *44*, 349−359. (c) Jakupec, M. A.; Galanski, M.; Arion, V. B.; Hartinger, C. G.; Keppler, B. K. Antitumour metal compounds: more than theme and variations. *Dalton Trans* **2008**, 183−194. (d) Albada, B.; Metzler-Nolte, N. Organometallic-Peptide bioconjugates: synthetic strategies and medicinal applications. *Chem. Rev.* **2016**, *116*, 11797−11839. (e) Zeng, L. L.; Gupta, P.; Chen, Y. L.; Wang, E. J.; Ji, L. N.; Chao, H.; Chen, Z. S. The development of anticancer ruthenium(II) complexes: from single molecule compounds to nanomaterials. *Chem. Soc. Rev.* **2017**, *46*, 5771−5804. (f) Hartinger, C. G.; Metzler-Nolte, N.; Dyson, P. J. Challenges and opportunities in the development of organometallic anticancer drugs. *Organometallics* **2012**, *31*, 5677−5685.

(3) (a) Weiss, A.; Berndsen, R. H.; Dubois, M.; Müller, C.; Schibli, R.; Griffioen, A. W.; Dyson, P. J.; Nowak-Sliwinska, P. In vivo anti-tumor activity of the organometallic ruthenium(II)-arene complex [Ru(η^6-*p*-cymene)-Cl_2(pta)] (RAPTA-C) in human ovarian and colorectal carcinomas. *Chem. Sci.* **2014**, *5*, 4742−4748. (b) Biancalana, L.; Zacchini, S.; Ferri, N.; Lupo, M. G.; Pampaloni, G.; Marchetti, F. Tuning the cytotoxicity of ruthenium(II) *para*-cymene complexes by mono-substitution at a triphenylphosphine/phenoxydiphenylphosphine ligand. *Dalton Trans* **2017**, *46*, 16589−16604. (c) Broomfield, L. M.; Alonso-Moreno, C.; Martin, E.; Shafir, A.; Posadas, I.; Cena, V.; Castro-Osma, J. A. Aminophosphine ligands as a privileged platform for development of antitumoral ruthenium(II) arene complexes. *Dalton trans* **2017**, *46*, 16113−16125.

(4) (a) Novohradsky, V.; Liu, Z.; Vojtiskova, M.; Sadler, P. J.; Brabec, V.; Kasparkova, J. Mechanism of cellular accumulation of an iridium(III) pentamethylcyclopentadienyl anticancer complex containing a C,N-chelating ligand. *Metallomics* **2014**, *6*, 682−690. (b) Liu, Z.; Salassa, L.; Habtemariam, A.; Pizarro, A. M.; Clarkson, G. J.; Sadler, P. J. Contrasting reactivity and cancer cell cytotoxicity of isoelectronic organometallic iridium(III) complexes. *Inorg. Chem.* **2011**, *50*, 5777−5783. (c) Liu, Z.; Romero-Canelon, I.; Habtemariam, A.; Clarkson, G. J.; Sadler, P. J. Potent half-sandwich iridium(III) anticancer complexes containing C^N-chelated and pyridine ligands. *Organometallics* **2014**, *33*, 5324−5333. (d) Liu, Z.; Habtemariam, A.; Pizarro, A. M.; Clarkson, G. J.; Sadler, P. J. Organometallic iridium(III) cyclopentadienyl anticancer complexes containing C,N-Chelating ligands. *Organometallics* **2011**, *30*, 4702−4710. (e) Yang, Y. L.; Guo, L.; Tian, Z. Z.; Liu, X. C.; Gong, Y. T.; Zheng, H. M.; Ge, X. X.; Liu, Z. Imine-N-heterocyclic carbene as versatile ligands in ruthenium(II) p-cymene anticancer complexes: a structure-activity relationship study. *Chem. - Asian J.*, **2018**, DOI: 10.1002/asia.201801058. (f) Yang, Y. L.; Guo, L.; Tian, Z. Z.; Gong, Y. T.; Zheng, H. M.; Zhang, S. M.; Xu, Z. S.; Ge, X. X.; Liu, Z. Novel and versatile imine-N-heterocyclic carbene half-sandwich iridium(III) complexes as lysosome-targeted anticancer agents. *Inorg. Chem.*, **2018**, DOI: 10.1021/acs.inorgchem.8b01656.

(5) (a) Liu, Z.; Habtemariam, A.; Pizarro, A. M.; Fletcher, S. A.; Kisova, A.; Vrana, O.; Salassa, L.; Bruijnincx, P. C.; Clarkson, G. J.; Brabec, V.; Sadler, P. J. Organometallic half-sandwich iridium anticancer complexes. *J. Med. Chem.* **2011**, *54*, 3011−3026. (b) Novohradsky, V.; Zerzankova, L.; Stepankova, J.; Kisova, A.; Kostrhunova, H.; Liu, Z.; Sadler, P. J.; Kasparkova, J.; Brabec, V. A dual-targeting, apoptosis-inducing organometallic half-sandwich iridium anticancer complex. *Metallomics* **2014**, *6*, 1491−1501. (c) Li, J. J.; Guo, L. H.; Tian, Z. Z.; Tian, M.; Zhang, S. M.; Xu, K.; Qian, Y. C.; Liu, Z. Novel half-sandwich iridium(III) imino-pyridyl complexes showing remarkable in vitro anticancer activity. *Dalton Trans* **2017**, *46*, 15520−15534.

(6) Meng, X.; Tang, G. R.; Jin, G. X. Vinyl and ring-opening metathesis polymerization of norbornene with novel half-sandwich iridium(III) complexes bearing hydroxyindanimine ligands. *Chem. Commun.* **2008**, 3178−3180.

(7) Li, J. J.; Tian, M.; Tian, Z. Z.; Zhang, S. M.; Yan, C.; Shao, C. F.; Liu, Z. Half-sandwich iridium(III) and ruthenium(II) complexes containing P^P-chelating ligands: a new class of potent anticancer agents with unusual redox features. *Inorg. Chem.* **2018**, *57*, 1705−1716.

(8) (a) Ludwig, G.; Mijatovic, S.; Randelovic, I.; Bulatovic, M.; Miljkovic, D.; Maksimovic-Ivanic, D.; Korb, M.; Lang, H.; Steinborn, D.; Kaluderovic, G. N. Biological activity of neutral and cationic iridium(III) complexes with κP and κP, κS coordinated Ph_2PCH_2S-$(O)_x$Ph (x = 0−2) ligands. *Eur. J. Med. Chem.* **2013**, *69*, 216−222. (b) Ludwig, G.; Kaluderovic, G. N.; Rüffer, T.; Bette, M.; Korb, M.; Block, M.; Paschke, R.; Lang, H.; Steinborn, D. Cationic arene ruthenium(II) complexes with chelating P-functionalized alkyl phenyl

DOI: 10.1021/acs.organomet.8b00402
Organometallics XXXX, XXX, XXX−XXX

sulfide and sulfoxide ligands as potent anticancer agents. *Dalton Trans* **2013**, *42*, 3771−3774.
(9) (a) Nakamura, A.; Anselment, T. M. J.; Claverie, J.; Goodall, B.; Jordan, R. F.; Mecking, S.; Rieger, B.; Sen, A.; Leeuwen, P. W. N. M. V.; Nozaki, K. *Ortho*-phosphinobenzenesulfonate: a Superb ligand for palladium-catalyzed coordination−insertion copolymerization of polar vinyl monomers. *Acc. Chem. Res.* **2013**, *46*, 1438−1449. (b) Sui, X. L.; Dai, S. Y.; Chen, C. L. Ethylene polymerization and copolymerization with polar monomers by cationic phosphine phosphonic amide palladium complexes. *ACS Catal.* **2015**, *5*, 5932−5937. (c) Guo, L. H.; Dai, S. Y.; Sui, X. L.; Chen, C. L. Palladium and nickel catalyzed chain walking olefin polymerization and copolymerization. *ACS Catal.* **2016**, *6*, 428−441. (d) Guo, L. H.; Liu, W. J.; Chen, C. L. Late transition metal catalyzed α-olefin polymerization and copolymerization with polar monomers. *Mater. Chem. Front.* **2017**, *1*, 2487−2494. (e) Xiong, S. Y.; Guo, L. H.; Zhang, S. M.; Liu, Z. Asymmetric cationic [P, O] type palladium complexes in olefin homopolymerization and copolymerization. *Chin. J. Chem.* **2017**, *35*, 1209−1221.
(10) Williams, D. B. G.; Evans, S. J.; de Bod, H.; Mokhadinyana, M. S.; Hughes, T. Directed ortho metallation chemistry and phosphine synthesis: new ligands for the suzuki-miyaura reaction. *Synthesis* **2009**, *2009*, 3106−3112.
(11) (a) Wang, C. L.; Liu, J. F.; Tian, Z. Z.; Tian, M.; Tian, L. J.; Zhao, W. Q.; Liu, Z. Half-sandwich iridium N-heterocyclic carbene anticancer complexes. *Dalton Trans* **2017**, *46*, 6870−6883. (b) Jensen, S. B.; Rodger, S. J.; Spicer, M. D. *J. Organomet. Chem.* **1998**, *556*, 151−158.
(12) Broomfield, L. M.; Alonso-Moreno, C.; Martin, E.; Shafir, A.; Posadas, I.; Ceña, V.; Castro-Osma, J. A. Aminophosphine ligands as a privileged platform for development of antitumoral ruthenium(II) arene complexes. *Dalton Trans* **2017**, *46*, 16113−16125.
(13) Trachootham, D.; Alexandre, J.; Huang, P. Targeting cancer cells by ROS-mediated mechanisms: a radical therapeutic approach? *Nat. Rev. Drug Discovery* **2009**, *8*, 579−591.
(14) Li, L.; Brennessel, W. W.; Jones, W. D. C−H activation of phenyl imines and 2-phenylpyridines with $[Cp^*MCl_2]_2$(M = Ir, Rh): regioselectivity, kinetics, and mechanism. *Organometallics* **2009**, *28*, 3492−3500.
(15) (a) Snelders, D. J. M.; Casini, A.; Edafe, F.; van Koten, G.; Klein Gebbink, R. J. M.; Dyson, P. J. Ruthenium(II) arene complexes with oligocationic triarylphosphine ligands: synthesis, DNA interactions and in vitro properties. *J. Organomet. Chem.* **2011**, *696*, 1108−1116. (b) Tian, M.; Li, J. J.; Zhang, S. M.; Guo, L. H.; He, X. D.; Kong, D. L.; Zhang, H. R.; Liu, Z. Half-sandwich ruthenium(II) complexes containing N^N-chelated imino-pyridyl ligands that are selectively toxic to cancer cells. *Chem. Commun.* **2017**, *53*, 12810−12813.
(16) Deubel, D. V.; Lau, J. K. C. In silico evolution of substrate selectivity: comparison of organometallic ruthenium complexes with the anticancer drug cisplatin. *Chem. Commun.* **2006**, 2451−2453.
(17) (a) Betanzos-Lara, S.; Liu, Z.; Habtemariam, A.; Pizarro, A. M.; Qamar, B.; Sadler, P. J. Organometallic ruthenium and iridium transfer-hydrogenation catalysts using coenzyme NADH as a cofactor. *Angew. Chem., Int. Ed.* **2012**, *51*, 3897−3900. (b) Liu, Z.; Deeth, R. J.; Butler, J. S.; Habtemariam, A.; Newton, M. E.; Sadler, P. J. Reduction of quinones by NADH catalyzed by organoiridium complexes. *Angew. Chem., Int. Ed.* **2013**, *52*, 4194−4197. (c) Liu, Z.; Romero-Canelon, I.; Qamar, B.; Hearn, J. M.; Habtemariam, A.; Barry, N. P. E.; Pizarro, A. M.; Clarkson, G. J.; Sadler, P. J. The potent oxidant anticancer activity of organoiridium catalysts. *Angew. Chem., Int. Ed.* **2014**, *53*, 3941−3946.
(18) (a) Rubbiani, R.; Can, S.; Kitanovic, I.; Alborzinia, H.; Stefanopoulou, M.; Kokoschka, M.; Monchgesang, S.; Sheldrick, W. S.; Wolfl, S.; Ott, I. Comparative in vitro evaluation of N-heterocyclic carbene gold(I) complexes of the benzimidazolylidene type. *J. Med. Chem.* **2011**, *54*, 8646−8657. (b) Kowol, C. R.; Heffeter, P.; Miklos, W.; Gille, L.; Trondl, R.; Cappellacci, L.; Berger, W.; Keppler, B. K. Mechanisms underlying reductant-induced reactive oxygen species formation by anticancer copper(II) compounds. *J. Biol. Inorg. Chem.* **2012**, *17*, 409−423.
(19) Belloc, F.; Belaud-Rotureau, M. A.; Lavignolle, V.; Bascans, E.; Braz-Pereira, E.; Durrieu, F.; Lacombe, F. Flow cytometry detection of caspase 3 activation in preapoptotic leukemic cells. *Cytometry* **2000**, *40*, 151−160.
(20) (a) Smiley, S. T.; Reers, M.; Mottola-Hartshorn, C.; Lin, M.; Chen, A.; Smith, T. W.; Steele, G. D., Jr.; Chen, L. B. Intracellular heterogeneity in mitochondrial membrane potentials revealed by a J-aggregate-forming lipophilic cation JC-1. *Proc. Natl. Acad. Sci. U. S. A.* **1991**, *88*, 3671−3675. (b) Zhang, H. R.; Guo, L. H.; Tian, Z. Z.; Tian, M.; Zhang, S. M.; Xu, Z. S.; Gong, P. W.; Zheng, X. F.; Zhao, J.; Liu, Z. Significant effects of counteranions on the anticancer activity of iridium(III) complexes. *Chem. Commun.* **2018**, *54*, 4421−4424.
(21) Boya, P.; Kroemer, G. Lysosomal membrane permeabilization in cell death. *Oncogene* **2008**, *27*, 6434−6451.
(22) Sun, B.; Liu, J.; Gao, Y.; Zheng, H. B.; Li, L.; Hu, Q. W.; Yuan, H. Q.; Lou, H. X. Design, synthesis and biological evaluation of nitrogen-containing macrocyclic bisbibenzyl derivatives as potent anticancer agents by targeting the lysosome. *Eur. J. Med. Chem.* **2017**, *136*, 603−618.

DOI: 10.1021/acs.organomet.8b00402
Organometallics XXXX, XXX, XXX−XXX